



Production of ${}^4\text{He}$ and ${}^4\overline{\text{He}}$ in Pb–Pb collisions at $\sqrt{s_{\text{NN}}} = 2.76$ TeV at the LHC

ALICE Collaboration *

Received 26 October 2017; received in revised form 20 December 2017; accepted 21 December 2017
Available online 27 December 2017

Abstract

Results on the production of ${}^4\text{He}$ and ${}^4\overline{\text{He}}$ nuclei in Pb–Pb collisions at $\sqrt{s_{\text{NN}}} = 2.76$ TeV in the rapidity range $|y| < 1$, using the ALICE detector, are presented in this paper. The rapidity densities corresponding to 0–10% central events are found to be $dN/dy_{{}^4\text{He}} = (0.8 \pm 0.4 \text{ (stat)} \pm 0.3 \text{ (syst)}) \times 10^{-6}$ and $dN/dy_{{}^4\overline{\text{He}}} = (1.1 \pm 0.4 \text{ (stat)} \pm 0.2 \text{ (syst)}) \times 10^{-6}$, respectively. This is in agreement with the statistical thermal model expectation assuming the same chemical freeze-out temperature ($T_{\text{chem}} = 156$ MeV) as for light hadrons. The measured ratio of ${}^4\overline{\text{He}}/{}^4\text{He}$ is $1.4 \pm 0.8 \text{ (stat)} \pm 0.5 \text{ (syst)}$.

© 2018 Elsevier B.V. This is an open access article under the CC BY license (<http://creativecommons.org/licenses/by/4.0/>).

Keywords: Pb–Pb collisions; ALICE detector; LHC; Anti-nuclei

1. Introduction

The production of light (hyper-)nuclei, up to a mass number $A = 3$, has been reported already in Pb–Pb collisions at $\sqrt{s_{\text{NN}}} = 2.76$ TeV at the Large Hadron Collider (LHC). This includes deuterons, ${}^3\text{He}$ and the hypertriton as well as their corresponding anti-particles [1,2]. The observed total yields can be described well by equilibrium thermal models [3–9], with only three free parameters: the chemical freeze-out temperature T_{chem} , the volume V and the baryo-chemical potential μ_B . The current best fit to the measured yields at the LHC, including results ranging in mass from pions up to ${}^3\text{He}$, results in a $T_{\text{chem}} = 156$ MeV [10]. The measurement of the production yields of ${}^4\text{He}$ and ${}^4\overline{\text{He}}$ ($A = 4$) will put additional constraints on T_{chem} . Since the baryo-chemical potential is consistent with zero ($\mu_B = 0.7 \pm 3.8$ MeV [11]) at LHC energies,

* E-mail address: alice-publications@cern.ch.

the expected anti-baryon to baryon ratio is unity. Therefore, also the ratio is expected to be close to unity for particles composed of (anti-)baryons, namely the anti-nuclei and nuclei [6].

Furthermore, ${}^4\overline{\text{He}}$ is the heaviest anti-nucleus ever observed. It was discovered in Au–Au collisions at RHIC by the STAR Collaboration [12]. Out of 10^9 Au–Au collisions at centre-of-mass energies per nucleon pair ($\sqrt{s_{\text{NN}}}$) of 200 GeV and 62.4 GeV, 18 ${}^4\overline{\text{He}}$ have been detected. The corresponding yield at a given transverse momentum p_{T} is compared to the prediction of the thermal model [13] and the coalescence nucleosynthesis model [14] and found to be consistent with both. A confirmation of this observation is still pending as no other experiment has been able to detect the ${}^4\overline{\text{He}}$ particle since then.

Coalescence models have been successfully used to describe the general trends of deuteron production [15–25] in relativistic nuclear collisions, albeit with a number of external parameters. These models are clearly challenged with the regular pattern observed in the production probability for light nuclei measured by the STAR [12] and ALICE [1] Collaborations. To extend the studies to $A = 4$ the measurement at LHC energies is obviously of great interest.

In this paper, the measurement of the production yield of the ${}^4\text{He}$ and ${}^4\overline{\text{He}}$ nuclei with the ALICE apparatus is presented. Besides the increase in collision energy, the main difference with respect to the measurement by the STAR Collaboration is the usage of a six layer silicon vertex detector in ALICE. Together with the other barrel detectors this provides precision information on vertex position, particle identification and momentum. The determined yields are compared to thermal model expectations.

2. Detector setup and data sample

The two main detectors involved in the identification of the ${}^4\text{He}$ and ${}^4\overline{\text{He}}$ particles are the Time Projection Chamber (TPC) [26] and the Time of Flight (TOF) detector [27], combined with the start time detector T0. In addition, V0 detectors ([28,29]) are used for centrality determination and the Inner Tracking System (ITS) [30] is employed for tracking and the discrimination between primary and secondary particles [1,31]. A full description of the ALICE detector can be found in [32], whereas the performance of the ALICE sub-detectors is reported in [33].

The measurement of the ${}^4\text{He}$ and ${}^4\overline{\text{He}}$ particles is performed on the 2011 data set of Pb–Pb collisions at $\sqrt{s_{\text{NN}}} = 2.76$ TeV. From this campaign, 38.7×10^6 events in a trigger mix of central, semi-central and minimum-bias events are used in this analysis. This leads to 20.7×10^6 events in the 0–10% centrality interval, 17.4×10^6 events in the 10–50% centrality interval and 0.6×10^6 events in the 50–80% centrality interval. The combined yields are extrapolated to the 0–10% centrality class with the procedure discussed in section 4.

3. Analysis

To ensure high tracking efficiency, high energy-deposit (dE/dx) resolution in the TPC and a good track matching between the TPC and TOF detectors, a set of selection criteria is applied. In order to select primary particles, the corresponding tracks have to originate from the primary vertex. The primary vertex position is estimated using the ITS and the TPC detectors. The resolution of the vertex determination is better than 50 μm in the xy-plane and 150 μm in the z-direction for charged particles with momenta above 1 GeV/c. To select primary tracks, the minimum distance from the vertex, called Distance-of-Closest-Approach (DCA), is required to be smaller than 1 cm along the z-axis, whereas the DCA in the xy-plane must not be greater than 0.1 cm. In addition, a hit in the TOF detector is required for a precise time measurement and only those tracks are used for the track reconstruction. The selection criteria are summarised in Table 1.

Table 1
Selection criteria applied for the ${}^4\text{He}$ and ${}^4\overline{\text{He}}$ analyses.

Track selection criteria	value
Number of clusters in TPC	$n_{\text{cl}} > 80$
Number of hits in ITS	$n_{\text{hits}} > 2$
TPC track quality	$\chi^2/\text{cluster} < 4$
Acceptance in pseudo-rapidity	$ \eta < 0.8$
Acceptance in rapidity	$ y < 1$
DCA _z	$\text{DCA}_z < 1\text{cm}$
DCA _{xy}	$\text{DCA}_{xy} < 0.1\text{cm}$
PID selection	value
TPC PID cut	$\pm 3\sigma$
TOF mass window	$\pm 3\sigma$

The dE/dx is measured in the TPC as a function of the rigidity p/z , where p is the momentum and z is the electric charge in units of the elementary charge e . This distribution of reconstructed charged particles is well described by the Bethe–Bloch formula [34,35] and is unique for each particle species.

Primarily, all events with at least one particle with a dE/dx corresponding to a ${}^3\text{He}$ and ${}^3\overline{\text{He}}$ or a higher mass are selected. To ensure a good track matching between the TPC and the TOF detectors, only candidates within 3 standard deviations (σ) around the mean in the dE/dx (TPC) vs. $\beta\gamma$ (TOF) plane are accepted. Here, β denotes the relativistic velocity $\beta = v/c$ and γ is the Lorentz factor. In order to select ${}^4\text{He}$ or ${}^4\overline{\text{He}}$ particles, candidates within a 3σ band of the Bethe–Bloch parametrisation in the dE/dx versus p/z distribution are taken into account. At higher momenta, the two Bethe–Bloch curves of ${}^4\text{He}$ or ${}^4\overline{\text{He}}$ and of ${}^3\text{He}$ or ${}^3\overline{\text{He}}$ approach each other. To study a possible contamination from ${}^3\text{He}$ and ${}^3\overline{\text{He}}$ particles, different narrower cuts for the TPC dE/dx selection band are investigated: while the upper cut of the band (3σ) is fixed, the lower cut is restricted progressively going in steps of 0.5 units from -3σ up to 0σ . For all these seven cuts the procedure described in the following is carried out and a yield dN/dy is determined.

In Fig. 1, the velocity (β) distributions of He candidates are plotted versus rigidity. One can clearly see the separation of ${}^3\text{He}$ and ${}^4\text{He}$. From these data, the m^2/z^2 (m = mass of the particle) distributions are calculated and displayed in the insert of this figure. From the insert, the separation of ${}^3\text{He}$ and ${}^4\text{He}$ can be quantitatively asserted. The m^2/z^2 is different for ${}^3\text{He}$ ($2.00\text{ GeV}^2/c^4$) and ${}^4\text{He}$ ($3.48\text{ GeV}^2/c^4$). Candidates lying within a window of $2.86\text{ GeV}^2/c^4 < m^2/z^2 < 4.87\text{ GeV}^2/c^4$ are identified as ${}^4\text{He}$ or ${}^4\overline{\text{He}}$ particles. This window is determined by a fit to the peak in the m^2/z^2 distribution of the selected tracks. Because of the low statistics, the fitting is done simultaneously both for particles and for anti-particles, including secondary ${}^4\text{He}$ knocked out from the material. A Gaussian with an exponential tail on the right side is used as the fit function. For the background, the sum of a first-order polynomial and an exponential shape is assumed. This is necessary to describe the time-signal shape of the TOF detector [27]. The polynomial shape is needed to cope with mismatched candidate tracks in the signal region. A similar procedure is used in [1].

For the analysis of positively charged ${}^4\text{He}$, contamination from ${}^4\text{He}$ nuclei which do not originate from the primary vertex, but stem from the detector material due to knockout processes, are taken into account. Monte Carlo studies suggest a cut on $p/z > 2\text{ GeV}/c$ to eliminate such

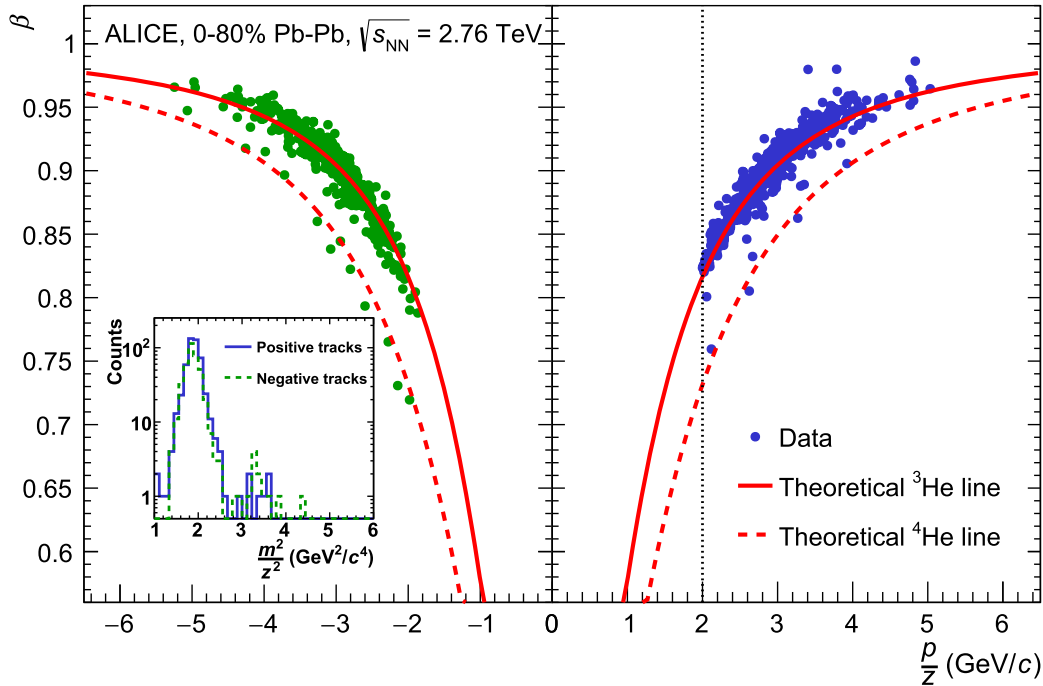


Fig. 1. Velocity β measured with the TOF detector as a function of the rigidity p/z . For this figure a selection band of -1.5 to 3σ around the mean of the TPC specific energy-loss distribution is required. Negatively (positively) charged particles are shown on the left (right) side, with positive tracks in blue and negative tracks in green. The dashed vertical line represents the cut on the rigidity $p/z = 2$ GeV/c (applied only for positively charged particles). The insert shows the m^2/z^2 distributions obtained from the data points shown in the main figure. (For interpretation of the references to colour in this figure legend, the reader is referred to the web version of this article.)

a background. Note that the background due to knockout processes is steeply falling with momentum and the signal is rising in this momentum range. Therefore, only ${}^4\text{He}$ candidates with a p/z greater than 2 GeV/c are accepted. The contamination at higher momenta is estimated to be a maximum of 0.13 counts out of a total count of the order of 10, which is added as a systematic uncertainty.

The small number of clear signal counts observed by combining the TPC and TOF information does not give any indication of background. In order to estimate an upper limit on the background counts from mismatched tracks in the TOF detector underneath the ${}^4\text{He}$ or ${}^4\overline{\text{He}}$ peak in the TOF mass window, a likelihood fit under the assumption of a flat background is performed in the dE/dx versus $\beta\gamma$ plane outside the $\pm 3\sigma$ matching band. In this way, background candidates are identified as mismatched particles. (These are usually rejected and only used for this purpose.) Due to limited statistics, this procedure cannot be used if a stronger selection criterion is applied for the TPC dE/dx selection, since no ${}^4\text{He}$ or ${}^4\overline{\text{He}}$ candidates are left to apply this technique. For these particular cases, we assume a constant ratio of ${}^3\text{He}$ to background counts and use this to estimate the number of ${}^4\text{He}$ background.

The background stemming from misidentification of (anti-) ${}^3\text{He}$ as (anti-) ${}^4\text{He}$ is estimated to be more than one order of magnitude smaller than the one from the mismatch of TPC tracks when extrapolated to the TOF detector and is therefore considered to be negligible. The estimated background decreases with more stringent TPC dE/dx cuts. The signal-to-background ratio improves depending on the tightness of the dE/dx cut from 1.7 to 8.4 for ${}^4\text{He}$ and from 1.7 to 17.6 for ${}^4\overline{\text{He}}$.

To estimate the efficiency for the detection of ${}^4\text{He}$ and ${}^4\overline{\text{He}}$, a Monte Carlo simulation is generated in which the kinematical distributions of the particles are generated flat both in rapidity

y and in transverse momentum p_T . The shape of p_T spectra in heavy-ion collisions is typically described by a blast-wave model [36]. This model assumes an average radial-flow velocity $\langle\beta\rangle$ and a kinetic freeze-out temperature T_{kin} as described in [37]. Generally, most hadron p_T spectra measured in heavy-ion collisions can be described well by one common set of parameters [38]. Surprisingly, this also works well for the description of deuteron and ${}^3\text{He}$ p_T spectra [1]. Hence the same prescription is used here for the p_T shape of ${}^4\text{He}$ and ${}^4\overline{\text{He}}$ particles, namely the same set of parameters is used, only the mass is changed to the ${}^4\text{He}$ mass.

Since only a small number of ${}^4\text{He}$ and ${}^4\overline{\text{He}}$ particles (14 ${}^4\overline{\text{He}}$ and 9 ${}^4\text{He}$ for the widest TPC dE/dx cut) are observed, a p_T spectrum can not be measured. It is estimated using the blast-wave parameters of deuterons and ${}^3\text{He}$ spectra [1]. The final acceptance \times efficiencies are obtained as described in [39] and are of the order of 15% for ${}^4\text{He}$ and 20% for ${}^4\overline{\text{He}}$. The difference originates from the 2 GeV/ c rigidity cut applied to ${}^4\text{He}$ candidates.

For the ${}^4\overline{\text{He}}$ analysis, the absorption in the detector material is taken into account using two different transport codes, namely GEANT3 [40] and GEANT4 [41]. These two codes use different models for the estimation of the absorption cross section. In GEANT4, a Glauber model based on the well known hadronic interaction cross sections for (anti-)protons is implemented [42]. The version of GEANT3 used in this analysis is modified [1] such that it calculates the absorption based on an empirical parameterisation [43], based on the measurements of anti-deuterons carried out at Serpukhov [44]. The baseline is given by the absorption calculated with GEANT4, while the GEANT3 based correction is used in the systematic uncertainty evaluation. The maximum absorption probability towards low p/z is about 20%. In contrast to GEANT4, which still shows an absorption of about 5% at $p_T = 10$ GeV/ c , GEANT3 exhibits basically no absorption above 3.5 GeV/ c .

The main contributions to the systematic uncertainty on the determined production yields are:

- The uncertainty due to the unknown shape of the p_T distributions, which is determined by using the blast-wave model based on the measured deuteron and ${}^3\text{He}$ spectra [1]. This leads to a systematic uncertainty contribution of around 13%.
- Only for ${}^4\text{He}$: The rigidity cut on p/z greater than 2 GeV/ c itself has a systematic uncertainty of 4 to 13% depending on the TPC PID cut. As mentioned before, the secondary contamination above this cut is estimated to be a maximum of 0.13 counts. This leads to a systematic uncertainty of at minimum 20% and at maximum 49% growing with stricter TPC PID cut. As the number of observed candidates shrinks with stricter TPC dE/dx selection, the systematic uncertainty on the secondary contamination grows.
- Only for ${}^4\overline{\text{He}}$: The absorption correction has an uncertainty of 7%, estimated from the difference of the two GEANT implementations.

Other systematic uncertainties are estimated by varying the cuts in the limits consistent with the detector resolution. The contributions of these systematic uncertainties are typically found to be below the percent range. The systematic uncertainty on the chosen TPC PID cut varies between 1% for the most loose cuts and 19% for stricter cuts. This is caused by the stronger sensitivity of the stricter cuts, namely the even further reduced low number of candidates, which is not reflected in the Monte Carlo simulation.

The final values and the corresponding uncertainties are calculated as a mean from the previously discussed variations of the selection criteria. The resulting systematic uncertainty on the final yield is 35% for ${}^4\text{He}$ and 20% for ${}^4\overline{\text{He}}$.

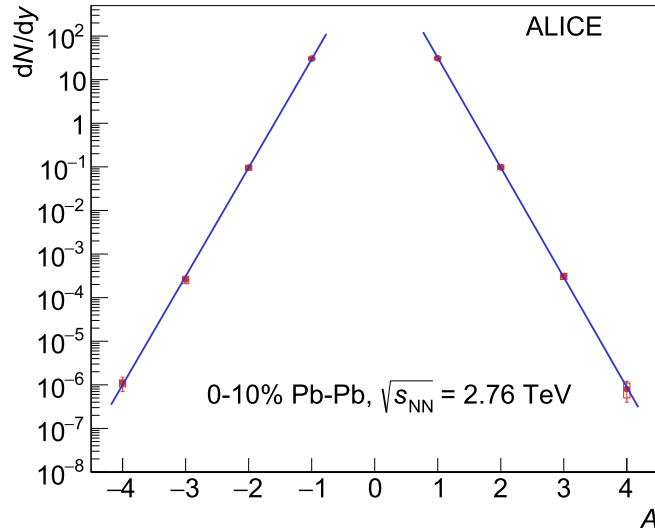


Fig. 2. dN/dy for protons ($A = 1$) up to ${}^4\text{He}$ ($A = 4$) and the corresponding anti-particles in central (0–10%) Pb–Pb collisions at $\sqrt{s_{\text{NN}}} = 2.76$ TeV. The blue lines are fits with an exponential function. Statistical uncertainties are shown as lines, whereas the systematic uncertainties are represented by boxes.

4. Results

The measurement is performed on a data set including central, semi-central and minimum-bias triggered events. To make use of all the data analysed, the semi-central and minimum-bias events have been extrapolated to 0–10% centrality interval assuming that the particle and anti-particle yields scale linearly with the charged-particle multiplicity $dN_{\text{ch}}/d\eta$. This procedure has already been tested to work well for the (anti-)hypertriton production [2]. In addition, d/p and ${}^3\text{He}/p$ ratios are measured to be approximately flat versus multiplicity within uncertainties [1]. Thus, for each centrality class, the number of analysed events is multiplied by the corresponding measured charged-particle density $dN_{\text{ch}}/d\eta$ [28]. If this is added up and divided by the total number of measured events it leads to a weighting factor of 1034. To get the final yield in the 0–10% centrality class the measured yield is multiplied with the $dN_{\text{ch}}/d\eta$ for 0–10% centrality (1447.5) and divided by the weighting factor, as $dN/dy_{0-10\%} = dN/dy_{\text{measured}} \times 1447.5/1034$.

This leads to final values of $dN/dy_{{}^4\text{He}} = (0.8 \pm 0.4 \text{ (stat)} \pm 0.3 \text{ (syst)}) \times 10^{-6}$ for ${}^4\text{He}$ and $dN/dy_{{}^4\overline{\text{He}}} = (1.1 \pm 0.4 \text{ (stat)} \pm 0.2 \text{ (syst)}) \times 10^{-6}$ for ${}^4\overline{\text{He}}$. For the ratio ${}^4\overline{\text{He}}/{}^4\text{He}$ we obtain $1.4 \pm 0.8 \text{ (stat)} \pm 0.5 \text{ (syst)}$ (“stat” and “syst” indicate the statistical and the systematic uncertainty).

The measured yields in the 0–10% centrality interval are shown in Fig. 2 together with those of (anti-)protons, (anti-)deuterons and (anti-) ${}^3\text{He}$ [1,38] (details on the extrapolation to 0–10% centrality can be found in [10]). The blue lines are exponential fits with the fit function Ke^{BA} resulting in $B = -5.8 \pm 0.2$, which corresponds to a penalty factor (suppression factor of production yield for nuclei with one additional baryon) of around 300. The same penalty factor is also obtained if the fit is done up to ${}^3\text{He}$ only [1].

The obtained penalty factor of around 300 for each additional nucleon is consistent with $T_{\text{chem}} \approx 160$ MeV in the equilibrium thermal models. The measured yields for ${}^4\text{He}$ and ${}^4\overline{\text{He}}$ nuclei are consistent with the predictions from the various (equilibrium) thermal models (THERMUS [45], GSI [5,46,47] and SHARE [48–50]) with $T_{\text{chem}} = 156$ MeV, as shown in Fig. 3 for complete statistical thermal model fits using the available light flavour data measured by the ALICE Collaboration. The fits in Fig. 3 extend the simple exponential model (Fig. 2) by incorporating Boltzmann statistics and degeneracy factors for all particles. If instead of all listed

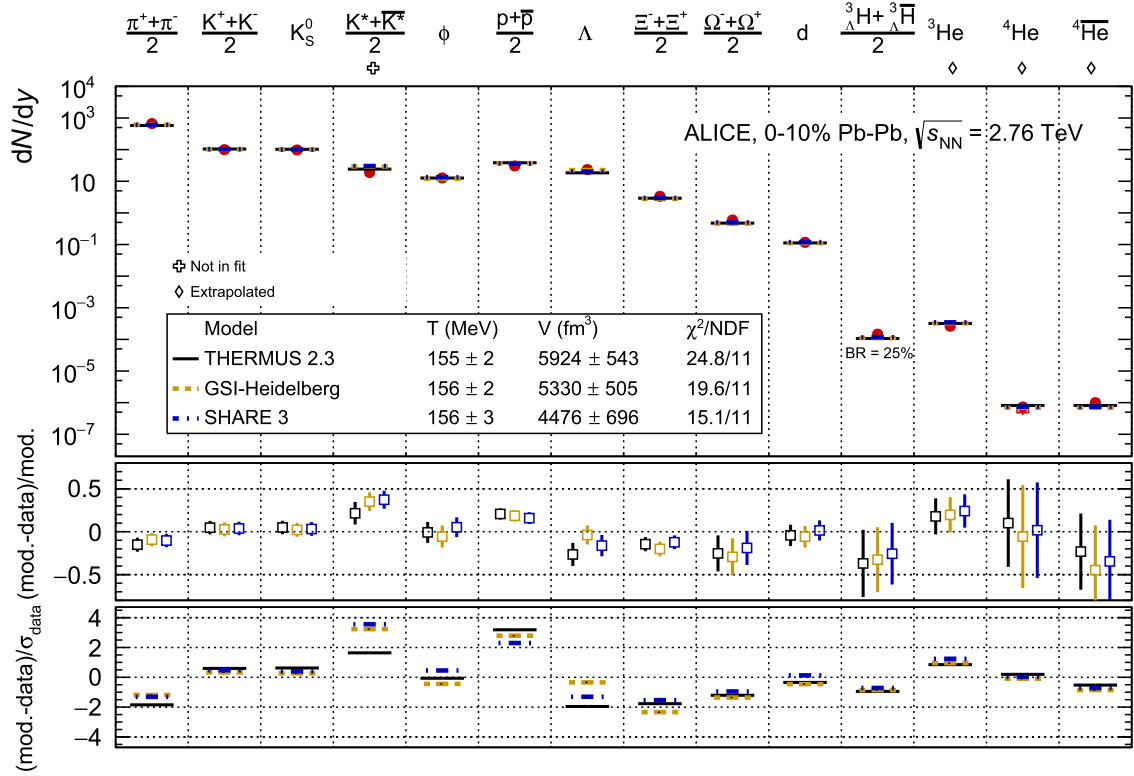


Fig. 3. Thermal model fits, with three different implementations, to the light flavour hadron yields in central (0–10%) Pb–Pb collisions at $\sqrt{s_{\text{NN}}} = 2.76$ TeV. The data points are taken from [1,2,38,51–54] and details of the fits can be found in [10,11]. The upper panel shows the fit results together with the data, whereas the middle panel shows the difference between model and data normalised to the model value and the lower panel the difference between model and data normalised to the experimental uncertainties.

particles only nuclei (deuterons, ${}^3\text{He}$ and ${}^4\text{He}$ and ${}^4\overline{\text{He}}$) are considered for the fit, the resulting temperatures are 154 ± 4 MeV. The pure measured yields for ${}^4\text{He}$ and ${}^4\overline{\text{He}}$ nuclei agree, depending on the model implementation, within the determined uncertainties with temperatures from 135 MeV to 177 MeV. Taken together these observations suggest that the relatively heavy ${}^4\text{He}$ and ${}^4\overline{\text{He}}$ nuclei are also produced statistically at the same temperature as the lighter particles.

5. Summary and conclusion

The ALICE Collaboration has measured the production yields of ${}^4\text{He}$ and ${}^4\overline{\text{He}}$ in central (0–10%) Pb–Pb collisions at $\sqrt{s_{\text{NN}}} = 2.76$ TeV. The ratio of the two yields is consistent with unity and the results are in good agreement with the prediction of the statistical thermal model assuming the same temperature of 156 MeV as is obtained from the fit to the other light flavour hadrons.

Data gathered at the current beam energy of $\sqrt{s_{\text{NN}}} = 5.02$ TeV in Pb–Pb collisions at the LHC (*Run 2*) will improve the studies described in this letter thanks to an increase in statistics by a factor of about 3. Based on the pilot measurement presented here, we conclude that a precision study will be possible in the data taking period starting from 2021 (*Run 3* of the LHC), where about 5500 ${}^4\text{He}$ (${}^4\overline{\text{He}}$) particles are expected to be reconstructed [55]. This will allow for the measurement of the transverse-momentum spectra. As the unknown shape of the p_{T} distributions is one of the major sources of the systematic uncertainty, the measurement of the spectrum will decrease the systematic uncertainty of the measured yield. As a consequence the precision of

the ratio of $^4\overline{\text{He}}/^4\text{He}$ will be significantly improved. In addition, a mass difference measurement similar to what was done in [56] will be possible.

Acknowledgements

The ALICE Collaboration would like to thank all its engineers and technicians for their invaluable contributions to the construction of the experiment and the CERN accelerator teams for the outstanding performance of the LHC complex. The ALICE Collaboration gratefully acknowledges the resources and support provided by all Grid centres and the Worldwide LHC Computing Grid (WLCG) collaboration. The ALICE Collaboration acknowledges the following funding agencies for their support in building and running the ALICE detector: A.I. Alikhanyan National Science Laboratory (Yerevan Physics Institute) Foundation (ANSL), State Committee of Science and World Federation of Scientists (WFS), Armenia; Austrian Academy of Sciences and Nationalstiftung für Forschung, Technologie und Entwicklung, Austria; Ministry of Communications and High Technologies, National Nuclear Research Center, Azerbaijan; Conselho Nacional de Desenvolvimento Científico e Tecnológico (CNPq), Universidade Federal do Rio Grande do Sul (UFRGS), Financiadora de Estudos e Projetos (Finep) and Fundação de Amparo à Pesquisa do Estado de São Paulo (FAPESP), Brazil; Ministry of Science & Technology of China (MSTC), National Natural Science Foundation of China (NSFC) and Ministry of Education of China (MOEC), China; Ministry of Science, Education and Sports and Croatian Science Foundation, Croatia; Ministry of Education, Youth and Sports of the Czech Republic, Czech Republic; The Danish Council for Independent Research – Natural Sciences, the Carlsberg Foundation and Danish National Research Foundation (DNRF), Denmark; Helsinki Institute of Physics (HIP), Finland; Commissariat à l’Energie Atomique (CEA) and Institut National de Physique Nucléaire et de Physique des Particules (IN2P3) and Centre National de la Recherche Scientifique (CNRS), France; Bundesministerium für Bildung, Wissenschaft, Forschung und Technologie (BMBF) and GSI Helmholtzzentrum für Schwerionenforschung GmbH, Germany; General Secretariat for Research and Technology, Ministry of Education, Research and Religions, Greece; National Research, Development and Innovation Office, Hungary; Department of Atomic Energy, Government of India (DAE), Department of Science and Technology, Government of India (DST), University Grants Commission, Government of India (UGC) and Council of Scientific and Industrial Research (CSIR), India; Indonesian Institute of Science, Indonesia; Centro Fermi – Museo Storico della Fisica e Centro Studi e Ricerche Enrico Fermi and Istituto Nazionale di Fisica Nucleare (INFN), Italy; Institute for Innovative Science and Technology, Nagasaki Institute of Applied Science (IIST), Japan Society for the Promotion of Science (JSPS) KAKENHI and Japanese Ministry of Education, Culture, Sports, Science and Technology (MEXT), Japan; Consejo Nacional de Ciencia y Tecnología (CONACYT), through Fondo de Cooperación Internacional en Ciencia y Tecnología (FONCICYT) and Dirección General de Asuntos del Personal Académico (DGAPA), Mexico; Nederlandse Organisatie voor Wetenschappelijk Onderzoek (NWO), Netherlands; The Research Council of Norway, Norway; Commission on Science and Technology for Sustainable Development in the South (COMSATS), Pakistan; Pontificia Universidad Católica del Perú, Peru; Ministry of Science and Higher Education and National Science Centre, Poland; Korea Institute of Science and Technology Information and National Research Foundation of Korea (NRF), Republic of Korea; Ministry of Education and Scientific Research, Institute of Atomic Physics and Romanian National Agency for Science, Technology and Innovation, Romania; Joint Institute for Nuclear Research (JINR), Ministry of Education and Science of the Russian Federation and National Research Centre Kurchatov Institute, Russia;

Ministry of Education, Science, Research and Sport of the Slovak Republic, Slovakia; National Research Foundation of South Africa, South Africa; Centro de Aplicaciones Tecnológicas y Desarrollo Nuclear (CEADEN), Cubaenergía, Cuba, Ministerio de Ciencia e Innovación and Centro de Investigaciones Energéticas, Medioambientales y Tecnológicas (CIEMAT), Spain; Swedish Research Council (VR) and Knut and Alice Wallenberg Foundation (KAW), Sweden; European Organization for Nuclear Research, Switzerland; National Science and Technology Development Agency (NSDTA), Suranaree University of Technology (SUT) and Office of the Higher Education Commission under NRU project of Thailand, Thailand; Turkish Atomic Energy Agency (TAEK), Turkey; National Academy of Sciences of Ukraine, Ukraine; Science and Technology Facilities Council (STFC), United Kingdom; National Science Foundation of the United States of America (NSF) and U.S. Department of Energy, Office of Nuclear Physics (DOE NP), United States of America.

References

- [1] ALICE Collaboration, J. Adam, et al., Production of light nuclei and anti-nuclei in pp and Pb–Pb collisions at LHC energies, *Phys. Rev. C* 93 (2016) 024917, <https://arxiv.org/abs/1506.08951v3>.
- [2] ALICE Collaboration, J. Adam, et al., ${}^3_{\Lambda}\text{H}$ and ${}^3_{\Lambda}\bar{\text{H}}$ production in Pb–Pb collisions at $\sqrt{s_{\text{NN}}} = 2.76$ TeV, *Phys. Lett. B* 754 (2016) 360, <https://arxiv.org/abs/1506.08453v2>.
- [3] P. Braun-Munzinger, J. Stachel, Production of strange clusters and strange matter in nucleus–nucleus collisions at the AGS, *J. Phys. G* 21 (1995) L17, <https://arxiv.org/abs/nucl-th/9412035v1>.
- [4] P. Braun-Munzinger, J. Stachel, Particle ratios, equilibration and the QCD phase boundary, *J. Phys. G* 28 (2002) 1971, <https://arxiv.org/abs/nucl-th/0112051v1>.
- [5] A. Andronic, P. Braun-Munzinger, J. Stachel, H. Stöcker, Production of light nuclei, hypernuclei and their antiparticles in relativistic nuclear collisions, *Phys. Lett. B* 697 (2011) 203, <https://arxiv.org/abs/1010.2995v2>.
- [6] J. Cleymans, S. Kabana, I. Kraus, H. Oeschler, K. Redlich, N. Sharma, Antimatter production in proton–proton and heavy-ion collisions at ultrarelativistic energies, *Phys. Rev. C* 84 (2011) 054916, <https://arxiv.org/abs/1105.3719v1>.
- [7] A. Andronic, P. Braun-Munzinger, K. Redlich, J. Stachel, The statistical model in Pb–Pb collisions at the LHC, *Nucl. Phys. A* 904 (2013) 535c, <https://arxiv.org/abs/1210.7724v1>.
- [8] J. Stachel, A. Andronic, P. Braun-Munzinger, K. Redlich, Confronting LHC data with the statistical hadronization model, *J. Phys. Conf. Ser.* 509 (2014) 012019, <https://arxiv.org/abs/1311.4662v1>.
- [9] J. Steinheimer, K. Gudima, A. Botvina, I. Mishustin, M. Bleicher, H. Stöcker, Hypernuclei, dibaryon and antinuclei production in high energy heavy ion collisions: thermal production vs. coalescence, *Phys. Lett. B* 714 (2012) 85, <https://arxiv.org/abs/1203.2547v2>.
- [10] M. Floris, Hadron yields and the phase diagram of strongly interacting matter, *Nucl. Phys. A* 931 (2014) 103, <https://arxiv.org/abs/1408.6403v3>.
- [11] A. Andronic, P. Braun-Munzinger, K. Redlich, J. Stachel, Hadron yields, the chemical freeze-out and the QCD phase diagram, *J. Phys. Conf. Ser.* 779 (2017) 012012, <https://arxiv.org/abs/1611.01347v2>.
- [12] STAR Collaboration, H. Agakishiev, et al., Observation of the antimatter helium-4 nucleus, *Nature* 473 (2011) 353, <https://arxiv.org/abs/1103.3312v2>, Erratum: *Nature* 475 (2011) 412.
- [13] P. Braun-Munzinger, J. Stachel, The quest for the quark–gluon plasma, *Nature* 448 (2007) 302.
- [14] H. Sato, K. Yazaki, On the coalescence model for high energy nuclear reactions, *Phys. Lett. B* 98 (1981) 153.
- [15] R. Hagedorn, Deuteron production in high-energy collisions, *Phys. Rev. Lett.* 5 (1960) 276–277.
- [16] S.T. Butler, C.A. Pearson, Deuterons from high-energy proton bombardment of matter, *Phys. Rev. Lett.* 7 (Jul 1961) 69–71, <https://doi.org/10.1103/PhysRevLett.7.69>.
- [17] S.T. Butler, C.A. Pearson, Deuterons from high-energy proton bombardment of matter, *Phys. Rev.* 129 (Jan 1963) 836–842, <https://doi.org/10.1103/PhysRev.129.836>.
- [18] J.L. Nagle, B.S. Kumar, D. Kusnezov, H. Sorge, R. Mattiello, Coalescence of deuterons in relativistic heavy ion collisions, *Phys. Rev. C* 53 (1996) 367–376.
- [19] R. Scheibl, U.W. Heinz, Coalescence and flow in ultrarelativistic heavy ion collisions, *Phys. Rev. C* 59 (1999) 1585–1602, [arXiv:nucl-th/9809092](https://arxiv.org/abs/nucl-th/9809092).
- [20] Y. Oh, Z.-W. Lin, C.M. Ko, Deuteron production and elliptic flow in relativistic heavy ion collisions, *Phys. Rev. C* 80 (Dec 2009) 064902, <https://doi.org/10.1103/PhysRevC.80.064902>.

- [21] L. Zhu, C.M. Ko, X. Yin, Light (anti-)nuclei production and flow in relativistic heavy-ion collisions, *Phys. Rev. C* 92 (6) (2015) 064911, [arXiv:1510.03568 \[nucl-th\]](https://arxiv.org/abs/1510.03568).
- [22] X. Yin, C.M. Ko, Y. Sun, L. Zhu, Elliptic flow of light nuclei, *Phys. Rev. C* 95 (5) (2017) 054913, [arXiv:1703.09383 \[nucl-th\]](https://arxiv.org/abs/1703.09383).
- [23] L. Zhu, H. Zheng, C.M. Ko, Y. Sun, Light nuclei production in Pb+Pb collisions at $\sqrt{s_{NN}} = 2.76$ TeV, [arXiv:1710.05139 \[nucl-th\]](https://arxiv.org/abs/1710.05139).
- [24] A.S. Botvina, J. Steinheimer, M. Bleicher, Formation of exotic baryon clusters in ultra-relativistic heavy-ion collisions, *Phys. Rev. C* 96 (1) (2017) 014913, [arXiv:1706.08335 \[nucl-th\]](https://arxiv.org/abs/1706.08335).
- [25] K.-J. Sun, L.-W. Chen, An analytical coalescence formula for particle production in relativistic heavy-ion collisions, [arXiv:1701.01935 \[nucl-th\]](https://arxiv.org/abs/1701.01935).
- [26] J. Alme, et al., The ALICE TPC, a large 3-dimensional tracking device with fast readout for ultra-high multiplicity events, *Nucl. Instrum. Methods A* 622 (2010) 316, <https://arxiv.org/abs/1001.1950v1>.
- [27] A. Akindinov, et al., Performance of the ALICE Time-Of-Flight detector at the LHC, *Eur. Phys. J. Plus* 128 (2013) 44.
- [28] ALICE Collaboration, K. Aamodt, et al., Centrality dependence of the charged-particle multiplicity density at midrapidity in Pb–Pb collisions at $\sqrt{s_{NN}} = 2.76$ TeV, *Phys. Rev. Lett.* 106 (2011) 032301, <https://arxiv.org/abs/1012.1657v2>.
- [29] ALICE Collaboration, B. Abelev, et al., Centrality determination of Pb–Pb collisions at $\sqrt{s_{NN}} = 2.76$ TeV with ALICE, *Phys. Rev. C* 88 (2013) 044909, <https://arxiv.org/abs/1301.4361v3>.
- [30] ALICE Collaboration, K. Aamodt, et al., Alignment of the ALICE Inner Tracking System with cosmic-ray tracks, *J. Instrum.* 5 (2010) P03003, <https://arxiv.org/abs/1001.0502v3>.
- [31] ALICE Collaboration, The ALICE definition of primary particles, <https://cds.cern.ch/record/2270008>.
- [32] ALICE Collaboration, K. Aamodt, et al., The ALICE experiment at the CERN LHC, *J. Instrum.* 3 (2008) S08002.
- [33] ALICE Collaboration, B. Abelev, et al., Performance of the ALICE experiment at the CERN LHC, *Int. J. Mod. Phys. A* 29 (2014) 1430044, <https://arxiv.org/abs/1402.4476v4>.
- [34] H. Bethe, Bremsformel für Elektronen relativistischer Geschwindigkeit, *Z. Phys.* 76 (1932) 293.
- [35] F. Bloch, Zur Bremsung rasch bewegter Teilchen beim Durchgang durch Materie, *Ann. Phys.* 408 (1933) 285.
- [36] E. Schnedermann, J. Sollfrank, U.W. Heinz, Thermal phenomenology of hadrons from 200-A/GeV S+S collisions, *Phys. Rev. C* 48 (1993) 2462, <https://arxiv.org/abs/nucl-th/9307020v1>.
- [37] ALICE Collaboration, B. Abelev, et al., Pion, kaon, and proton production in central Pb–Pb collisions at $\sqrt{s_{NN}} = 2.76$ TeV, *Phys. Rev. Lett.* 109 (2012) 252301, <https://arxiv.org/abs/1208.1974v3>.
- [38] ALICE Collaboration, B. Abelev, et al., Centrality dependence of π , K, p production in Pb–Pb collisions at $\sqrt{s_{NN}} = 2.76$ TeV, *Phys. Rev. C* 88 (2013) 044910, <https://arxiv.org/abs/1303.0737v3>.
- [39] ALICE Collaboration, J. Adam, et al., Search for weakly decaying $\bar{\Lambda}n$ and $\Lambda\Lambda$ exotic bound states in central Pb–Pb collisions at $\sqrt{s_{NN}} = 2.76$ TeV, *Phys. Lett. B* 752 (2016) 267, <https://arxiv.org/abs/1506.07499v2>.
- [40] R. Brun, F. Carminati, S. Giani, GEANT Detector Description and Simulation Tool, CERN-W5013, CERN-W-5013, 1994.
- [41] S. Agostinelli, et al., GEANT 4: a simulation toolkit, *Nucl. Instrum. Methods A* 506 (2003) 250.
- [42] V. Uzhinsky, et al., Antinucleus–nucleus cross sections implemented in geant4, *Phys. Lett. B* 705 (2011) 235.
- [43] A.A. Moiseev, J.F. Ormes, Inelastic cross section for antihelium on nuclei: an empirical formula for use in the experiments to search for cosmic antimatter, *Astropart. Phys.* 6 (1997) 379.
- [44] V.V. Abramov, et al., Production of deuterons and antideuterons with large pt in pp and pA collisions at 70 GeV, *Yad. Fiz.* 45 (1987) 1362.
- [45] S. Wheaton, J. Cleymans, M. Hauer, THERMUS – a thermal model package for ROOT, *Comput. Phys. Commun.* 180 (2009) 84, <https://arxiv.org/abs/hep-ph/0407174v2>.
- [46] A. Andronic, P. Braun-Munzinger, J. Stachel, Thermal hadron production in relativistic nuclear collisions: the hadron mass spectrum, the horn, and the QCD phase transition, *Phys. Lett. B* 673 (2009) 142, <https://arxiv.org/abs/0812.1186v3>, Erratum: *Phys. Lett. B* 678 (2009) 516.
- [47] A. Andronic, P. Braun-Munzinger, K. Redlich, J. Stachel, Decoding the phase structure of QCD via particle production at high energy, [arXiv:1710.09425 \[nucl-th\]](https://arxiv.org/abs/1710.09425).
- [48] G. Torrieri, S. Steinke, W. Broniowski, W. Florkowski, J. Letessier, J. Rafelski, SHARE: statistical hadronization with resonances, *Comput. Phys. Commun.* 167 (2005) 229, <https://arxiv.org/abs/nucl-th/0404083v2>.
- [49] G. Torrieri, S. Jeon, J. Letessier, J. Rafelski, SHAREv2: fluctuations and a comprehensive treatment of decay feed-down, *Comput. Phys. Commun.* 175 (2006) 635, <https://arxiv.org/abs/nucl-th/0603026v2>.
- [50] M. Petran, J. Letessier, J. Rafelski, G. Torrieri, SHARE with CHARM, *Comput. Phys. Commun.* 185 (2014) 2056, <https://arxiv.org/abs/1310.5108v2>.

- [51] ALICE Collaboration, B. Abelev, et al., K_s^0 and Λ production in Pb–Pb collisions at $\sqrt{s_{\text{NN}}} = 2.76$ TeV, Phys. Rev. Lett. 111 (2013) 222301, <https://arxiv.org/abs/1307.5530v2>.
- [52] ALICE Collaboration, B. Abelev, et al., Multi-strange baryon production at mid-rapidity in Pb–Pb collisions at $\sqrt{s_{\text{NN}}} = 2.76$ TeV, Phys. Lett. B 728 (2014) 216, <https://arxiv.org/abs/1307.5543v3>.
- [53] ALICE Collaboration, B. Abelev, et al., $K^*(892)^0$ and $\phi(1020)$ production in Pb–Pb collisions at $\sqrt{s_{\text{NN}}} = 2.76$ TeV, Phys. Rev. C 91 (2015) 024609, <https://arxiv.org/abs/1404.0495v3>.
- [54] ALICE Collaboration, J. Adam, et al., $K^*(892)^0$ and $\phi(1020)$ meson production at high transverse momentum in pp and Pb–Pb collisions at $\sqrt{s_{\text{NN}}} = 2.76$ TeV, Phys. Rev. C 95 (2017) 064606, arXiv:1702.00555 [nucl-ex].
- [55] ALICE Collaboration, B. Abelev, et al., Upgrade of the ALICE experiment: letter of intent, J. Phys. G, Nucl. Part. Phys. 41 (2014) 087001.
- [56] ALICE Collaboration, J. Adam, et al., Precision measurement of the mass difference between light nuclei and anti-nuclei, Nat. Phys. 11 (2015) 811, <https://arxiv.org/abs/1508.03986v1>.

ALICE Collaboration

S. Acharya¹³⁷, D. Adamová⁹⁴, J. Adolfsson³⁴, M.M. Aggarwal⁹⁹,
 G. Aglieri Rinella³⁵, M. Agnello³¹, N. Agrawal⁴⁸, Z. Ahammed¹³⁷,
 S.U. Ahn⁷⁹, S. Aiola¹⁴¹, A. Akindinov⁶⁴, M. Al-Turany¹⁰⁶,
 S.N. Alam¹³⁷, D.S.D. Albuquerque¹²², D. Aleksandrov⁹⁰,
 B. Alessandro⁵⁸, R. Alfaro Molina⁷⁴, Y. Ali¹⁵, A. Alici^{12,53,27}, A. Alkin³,
 J. Alme²², T. Alt⁷⁰, L. Altenkamper²², I. Altsybeev¹³⁶,
 C. Alves Garcia Prado¹²¹, C. Andrei⁸⁷, D. Andreou³⁵, H.A. Andrews¹¹⁰,
 A. Andronic¹⁰⁶, V. Anguelov¹⁰⁴, C. Anson⁹⁷, T. Antičić¹⁰⁷, F. Antinori⁵⁶,
 P. Antonioli⁵³, L. Aphecetche¹¹⁴, H. Appelshäuser⁷⁰, S. Arcelli²⁷,
 R. Arnaldi⁵⁸, O.W. Arnold^{105,36}, I.C. Arsene²¹, M. Arslanok¹⁰⁴,
 B. Audurier¹¹⁴, A. Augustinus³⁵, R. Auerbeck¹⁰⁶, M.D. Azmi¹⁷,
 A. Badalà⁵⁵, Y.W. Baek^{60,78}, S. Bagnasco⁵⁸, R. Bailhache⁷⁰, R. Bala¹⁰¹,
 A. Baldisseri⁷⁵, M. Ball⁴⁵, R.C. Baral^{67,88}, A.M. Barbano²⁶,
 R. Barbera²⁸, F. Barile³³, L. Barioglio²⁶, G.G. Barnaföldi¹⁴⁰,
 L.S. Barnby⁹³, V. Barret¹³¹, P. Bartalini⁷, K. Barth³⁵, E. Bartsch⁷⁰,
 N. Bastid¹³¹, S. Basu¹³⁹, G. Batigne¹¹⁴, B. Batyunya⁷⁷, P.C. Batzing²¹,
 J.L. Bazo Alba¹¹¹, I.G. Bearden⁹¹, H. Beck¹⁰⁴, C. Bedda⁶³,
 N.K. Behera⁶⁰, I. Belikov¹³³, F. Bellini^{27,35}, H. Bello Martinez²,
 R. Bellwied¹²⁴, L.G.E. Beltran¹²⁰, V. Belyaev⁸³, G. Bencedi¹⁴⁰,
 S. Beole²⁶, A. Bercuci⁸⁷, Y. Berdnikov⁹⁶, D. Berenyi¹⁴⁰, R.A. Bertens¹²⁷,
 D. Berzano³⁵, L. Betev³⁵, A. Bhasin¹⁰¹, I.R. Bhat¹⁰¹, B. Bhattacharjee⁴⁴,
 J. Bhom¹¹⁸, A. Bianchi²⁶, L. Bianchi¹²⁴, N. Bianchi⁵¹, C. Bianchin¹³⁹,
 J. Bielčik³⁹, J. Bielčíková⁹⁴, A. Bilandzic^{36,105}, G. Biro¹⁴⁰, R. Biswas⁴,
 S. Biswas⁴, J.T. Blair¹¹⁹, D. Blau⁹⁰, C. Blume⁷⁰, G. Boca¹³⁴, F. Bock³⁵,
 A. Bogdanov⁸³, L. Boldizsár¹⁴⁰, M. Bombara⁴⁰, G. Bonomi¹³⁵,
 M. Bonora³⁵, J. Book⁷⁰, H. Borel⁷⁵, A. Borissov^{104,19}, M. Borri¹²⁶,
 E. Botta²⁶, C. Bourjau⁹¹, L. Bratrud⁷⁰, P. Braun-Munzinger¹⁰⁶,

M. Bregant¹²¹, T.A. Broker⁷⁰, M. Broz³⁹, E.J. Brucken⁴⁶, E. Bruna⁵⁸,
 G.E. Bruno^{35,33}, D. Budnikov¹⁰⁸, H. Buesching⁷⁰, S. Bufalino³¹,
 P. Buhler¹¹³, P. Buncic³⁵, O. Busch¹³⁰, Z. Buthelezi⁷⁶, J.B. Butt¹⁵,
 J.T. Buxton¹⁸, J. Cabala¹¹⁶, D. Caffarri^{35,92}, H. Caines¹⁴¹, A. Caliva^{63,106},
 E. Calvo Villar¹¹¹, P. Camerini²⁵, A.A. Capon¹¹³, F. Carena³⁵,
 W. Carena³⁵, F. Carnesecchi^{27,12}, J. Castillo Castellanos⁷⁵, A.J. Castro¹²⁷,
 E.A.R. Casula⁵⁴, C. Ceballos Sanchez⁹, S. Chandra¹³⁷, B. Chang¹²⁵,
 W. Chang⁷, S. Chapeland³⁵, M. Chartier¹²⁶, S. Chattopadhyay¹³⁷,
 S. Chattopadhyay¹⁰⁹, A. Chauvin^{36,105}, C. Cheshkov¹³², B. Cheynis¹³²,
 V. Chibante Barroso³⁵, D.D. Chinellato¹²², S. Cho⁶⁰, P. Chochula³⁵,
 M. Chojnacki⁹¹, S. Choudhury¹³⁷, T. Chowdhury¹³¹, P. Christakoglou⁹²,
 C.H. Christensen⁹¹, P. Christiansen³⁴, T. Chujo¹³⁰, S.U. Chung¹⁹,
 C. Cicalo⁵⁴, L. Cifarelli^{12,27}, F. Cindolo⁵³, J. Cleymans¹⁰⁰,
 F. Colamaria^{52,33}, D. Colella^{35,52,65}, A. Collu⁸², M. Colocci²⁷,
 M. Concas^{58,ii}, G. Conesa Balbastre⁸¹, Z. Conesa del Valle⁶¹,
 J.G. Contreras³⁹, T.M. Cormier⁹⁵, Y. Corrales Morales⁵⁸,
 I. Cortés Maldonado², P. Cortese³², M.R. Cosentino¹²³, F. Costa³⁵,
 S. Costanza¹³⁴, J. Crkovská⁶¹, P. Crochet¹³¹, E. Cuautle⁷²,
 L. Cunqueiro^{95,71}, T. Dahms^{36,105}, A. Dainese⁵⁶, M.C. Danisch¹⁰⁴,
 A. Danu⁶⁸, D. Das¹⁰⁹, I. Das¹⁰⁹, S. Das⁴, A. Dash⁸⁸, S. Dash⁴⁸, S. De⁴⁹,
 A. De Caro³⁰, G. de Cataldo⁵², C. de Conti¹²¹, J. de Cuveland⁴²,
 A. De Falco²⁴, D. De Gruttola^{30,12}, N. De Marco⁵⁸, S. De Pasquale³⁰,
 R.D. De Souza¹²², H.F. Degenhardt¹²¹, A. Deisting^{106,104}, A. Deloff⁸⁶,
 C. Deplano⁹², P. Dhankher⁴⁸, D. Di Bari³³, A. Di Mauro³⁵,
 P. Di Nezza⁵¹, B. Di Ruzza⁵⁶, M.A. Diaz Corchero¹⁰, T. Dietel¹⁰⁰,
 P. Dillenseger⁷⁰, Y. Ding⁷, R. Divià³⁵, Ø. Djuvsland²², A. Dobrin³⁵,
 D. Domenicis Gimenez¹²¹, B. Dönigus⁷⁰, O. Dordic²¹,
 L.V.R. Doremalen⁶³, A.K. Dubey¹³⁷, A. Dubla¹⁰⁶, L. Ducroux¹³²,
 S. Dudi⁹⁹, A.K. Duggal⁹⁹, M. Dukhishyam⁸⁸, P. Dupieux¹³¹,
 R.J. Ehlers¹⁴¹, D. Elia⁵², E. Endress¹¹¹, H. Engel⁶⁹, E. Eppele¹⁴¹,
 B. Erasmus¹¹⁴, F. Erhardt⁹⁸, B. Espagnon⁶¹, G. Eulisse³⁵, J. Eum¹⁹,
 D. Evans¹¹⁰, S. Evdokimov¹¹², L. Fabbietti^{105,36}, J. Faivre⁸¹,
 A. Fantoni⁵¹, M. Fasel⁹⁵, L. Feldkamp⁷¹, A. Feliciello⁵⁸, G. Feofilov¹³⁶,
 A. Fernández Téllez², E.G. Ferreira¹⁶, A. Ferretti²⁶, A. Festanti^{29,35},
 V.J.G. Feuillard^{75,131}, J. Figiel¹¹⁸, M.A.S. Figueredo¹²¹, S. Filchagin¹⁰⁸,
 D. Finogeev⁶², F.M. Fionda^{22,24}, M. Floris³⁵, S. Foertsch⁷⁶, P. Foka¹⁰⁶,
 S. Fokin⁹⁰, E. Fragiaco⁵⁹, A. Francescon³⁵, A. Francisco¹¹⁴,

U. Frankenfeld¹⁰⁶, G.G. Fronze²⁶, U. Fuchs³⁵, C. Furget⁸¹, A. Furs⁶²,
 M. Fusco Girard³⁰, J.J. Gaardhøje⁹¹, M. Gagliardi²⁶, A.M. Gago¹¹¹,
 K. Gajdosova⁹¹, M. Gallio²⁶, C.D. Galvan¹²⁰, P. Ganoti⁸⁵,
 C. Garabatos¹⁰⁶, E. Garcia-Solis¹³, K. Garg²⁸, C. Gargiulo³⁵,
 P. Gasik^{105,36}, E.F. Gauger¹¹⁹, M.B. Gay Ducati⁷³, M. Germain¹¹⁴,
 J. Ghosh¹⁰⁹, P. Ghosh¹³⁷, S.K. Ghosh⁴, P. Gianotti⁵¹,
 P. Giubellino^{35,106,58}, P. Giubilato²⁹, E. Gladysz-Dziadus¹¹⁸, P. Glässel¹⁰⁴,
 D.M. Gómez Coral⁷⁴, A. Gomez Ramirez⁶⁹, A.S. Gonzalez³⁵,
 V. Gonzalez¹⁰, P. González-Zamora^{10,2}, S. Gorbunov⁴², L. Görlich¹¹⁸,
 S. Gotovac¹¹⁷, V. Grabski⁷⁴, L.K. Graczykowski¹³⁸, K.L. Graham¹¹⁰,
 L. Greiner⁸², A. Grelli⁶³, C. Grigoras³⁵, V. Grigoriev⁸³, A. Grigoryan¹,
 S. Grigoryan⁷⁷, J.M. Gronefeld¹⁰⁶, F. Grosa³¹, J.F. Grosse-Oetringhaus³⁵,
 R. Grosso¹⁰⁶, F. Guber⁶², R. Guernane⁸¹, B. Guerzoni²⁷,
 K. Gulbrandsen⁹¹, T. Gunji¹²⁹, A. Gupta¹⁰¹, R. Gupta¹⁰¹, I.B. Guzman²,
 R. Haake³⁵, C. Hadjidakis⁶¹, H. Hamagaki⁸⁴, G. Hamar¹⁴⁰,
 J.C. Hamon¹³³, M.R. Haque⁶³, J.W. Harris¹⁴¹, A. Harton¹³, H. Hassan⁸¹,
 D. Hatzifotiadou^{12,53}, S. Hayashi¹²⁹, S.T. Heckel⁷⁰, E. Hellbär⁷⁰,
 H. Helstrup³⁷, A. Herghelegiu⁸⁷, E.G. Hernandez², G. Herrera Corral¹¹,
 F. Herrmann⁷¹, B.A. Hess¹⁰³, K.F. Hetland³⁷, H. Hillemanns³⁵,
 C. Hills¹²⁶, B. Hippolyte¹³³, B. Hohlweger¹⁰⁵, D. Horak³⁹,
 S. Hornung¹⁰⁶, R. Hosokawa^{81,130}, P. Hristov³⁵, C. Hughes¹²⁷,
 T.J. Humanic¹⁸, N. Hussain⁴⁴, T. Hussain¹⁷, D. Hutter⁴², D.S. Hwang²⁰,
 S.A. Iga Buitron⁷², R. Ilkaev¹⁰⁸, M. Inaba¹³⁰, M. Ippolitov^{83,90},
 M.S. Islam¹⁰⁹, M. Ivanov¹⁰⁶, V. Ivanov⁹⁶, V. Izucheev¹¹², B. Jacak⁸²,
 N. Jacazio²⁷, P.M. Jacobs⁸², M.B. Jadhav⁴⁸, S. Jadlovská¹¹⁶,
 J. Jadlovsky¹¹⁶, S. Jaelani⁶³, C. Jahnke³⁶, M.J. Jakubowska¹³⁸,
 M.A. Janik¹³⁸, P.H.S.Y. Jayarathna¹²⁴, C. Jena⁸⁸, M. Jercic⁹⁸,
 R.T. Jimenez Bustamante¹⁰⁶, P.G. Jones¹¹⁰, A. Jusko¹¹⁰, P. Kalinak⁶⁵,
 A. Kalweit³⁵, J.H. Kang¹⁴², V. Kaplin⁸³, S. Kar¹³⁷, A. Karasu Uysal⁸⁰,
 O. Karavichev⁶², T. Karavicheva⁶², L. Karayan^{106,104}, P. Karczmarczyk³⁵,
 E. Karpechev⁶², U. Kebschull⁶⁹, R. Keidel¹⁴³, D.L.D. Keijdener⁶³,
 M. Keil³⁵, B. Ketzer⁴⁵, Z. Khabanova⁹², P. Khan¹⁰⁹, S.A. Khan¹³⁷,
 A. Khanzadeev⁹⁶, Y. Kharlov¹¹², A. Khatun¹⁷, A. Khuntia⁴⁹,
 M.M. Kielbowicz¹¹⁸, B. Kileng³⁷, B. Kim¹³⁰, D. Kim¹⁴², D.J. Kim¹²⁵,
 H. Kim¹⁴², J.S. Kim⁴³, J. Kim¹⁰⁴, M. Kim⁶⁰, S. Kim²⁰, T. Kim¹⁴²,
 S. Kirsch⁴², I. Kisel⁴², S. Kiselev⁶⁴, A. Kisiel¹³⁸, G. Kiss¹⁴⁰, J.L. Klay⁶,
 C. Klein⁷⁰, J. Klein³⁵, C. Klein-Bösing⁷¹, S. Klewin¹⁰⁴, A. Kluge³⁵,

M.L. Knichel^{104,35}, A.G. Knospe¹²⁴, C. Kobdaj¹¹⁵, M. Kofarago¹⁴⁰,
 M.K. Köhler¹⁰⁴, T. Kollegger¹⁰⁶, V. Kondratiev¹³⁶, N. Kondratyeva⁸³,
 E. Kondratyuk¹¹², A. Konevskikh⁶², M. Konyushikhin¹³⁹, M. Kopcik¹¹⁶,
 M. Kour¹⁰¹, C. Kouzinopoulos³⁵, O. Kovalenko⁸⁶, V. Kovalenko¹³⁶,
 M. Kowalski¹¹⁸, G. Koyithatta Meethalevedu⁴⁸, I. Králik⁶⁵,
 A. Kravčáková⁴⁰, L. Kreis¹⁰⁶, M. Krivda^{110,65}, F. Krizek⁹⁴, E. Kryshen⁹⁶,
 M. Krzewicki⁴², A.M. Kubera¹⁸, V. Kučera⁹⁴, C. Kuhn¹³³, P.G. Kuijer⁹²,
 A. Kumar¹⁰¹, J. Kumar⁴⁸, L. Kumar⁹⁹, S. Kumar⁴⁸, S. Kundu⁸⁸,
 P. Kurashvili⁸⁶, A. Kurepin⁶², A.B. Kurepin⁶², A. Kuryakin¹⁰⁸,
 S. Kushpil⁹⁴, M.J. Kweon⁶⁰, Y. Kwon¹⁴², S.L. La Pointe⁴²,
 P. La Rocca²⁸, C. Lagana Fernandes¹²¹, Y.S. Lai⁸², I. Lakomov³⁵,
 R. Langoy⁴¹, K. Lapidus¹⁴¹, C. Lara⁶⁹, A. Lardeux²¹, A. Lattuca²⁶,
 E. Laudi³⁵, R. Lavicka³⁹, R. Lea²⁵, L. Leardini¹⁰⁴, S. Lee¹⁴², F. Lehas⁹²,
 S. Lehner¹¹³, J. Lehrbach⁴², R.C. Lemmon⁹³, E. Leogrande⁶³,
 I. León Monzón¹²⁰, P. Lévai¹⁴⁰, X. Li¹⁴, J. Lien⁴¹, R. Lietava¹¹⁰,
 B. Lim¹⁹, S. Lindal²¹, V. Lindenstruth⁴², S.W. Lindsay¹²⁶,
 C. Lippmann¹⁰⁶, M.A. Lisa¹⁸, V. Litichevskiy⁴⁶, W.J. Llope¹³⁹,
 D.F. Lodato⁶³, P.I. Loenne²², V. Loginov⁸³, C. Loizides^{95,82},
 P. Loncar¹¹⁷, X. Lopez¹³¹, E. López Torres⁹, A. Lowe¹⁴⁰, P. Luettig⁷⁰,
 J.R. Luhder⁷¹, M. Lunardon²⁹, G. Luparello^{59,25}, M. Lupi³⁵,
 T.H. Lutz¹⁴¹, A. Maevskaya⁶², M. Mager³⁵, S.M. Mahmood²¹,
 A. Maire¹³³, R.D. Majka¹⁴¹, M. Malaev⁹⁶, L. Malinina^{77,iii},
 D. Mal'Kevich⁶⁴, P. Malzacher¹⁰⁶, A. Mamonov¹⁰⁸, V. Manko⁹⁰,
 F. Manso¹³¹, V. Manzari⁵², Y. Mao⁷, M. Marchisone^{132,76,128}, J. Mareš⁶⁶,
 G.V. Margagliotti²⁵, A. Margotti⁵³, J. Margutti⁶³, A. Marín¹⁰⁶,
 C. Markert¹¹⁹, M. Marquard⁷⁰, N.A. Martin¹⁰⁶, P. Martinengo³⁵,
 J.A.L. Martinez⁶⁹, M.I. Martínez², G. Martínez García¹¹⁴,
 M. Martinez Pedreira³⁵, S. Masciocchi¹⁰⁶, M. Maserà²⁶, A. Masoni⁵⁴,
 E. Masson¹¹⁴, A. Mastroserio⁵², A.M. Mathis^{105,36}, P.F.T. Matuoka¹²¹,
 A. Matyja¹²⁷, C. Mayer¹¹⁸, J. Mazer¹²⁷, M. Mazzilli³³, M.A. Mazzoni⁵⁷,
 F. Meddi²³, Y. Melikyan⁸³, A. Menchaca-Rocha⁷⁴, E. Meninno³⁰,
 J. Mercado Pérez¹⁰⁴, M. Meres³⁸, S. Mhlanga¹⁰⁰, Y. Miake¹³⁰,
 M.M. Mieskolainen⁴⁶, D.L. Mihaylov¹⁰⁵, K. Mikhaylov^{77,64},
 A. Mischke⁶³, A.N. Mishra⁴⁹, D. Miśkowiec¹⁰⁶, J. Mitra¹³⁷, C.M. Mitu⁶⁸,
 N. Mohammadi⁶³, A.P. Mohanty⁶³, B. Mohanty⁸⁸, M. Mohisin Khan^{17,iv},
 E. Montes¹⁰, D.A. Moreira De Godoy⁷¹, L.A.P. Moreno², S. Moretto²⁹,
 A. Morreale¹¹⁴, A. Morsch³⁵, V. Muccifora⁵¹, E. Mudnic¹¹⁷,

D. Mühlheim⁷¹, S. Muhuri¹³⁷, J.D. Mulligan¹⁴¹, M.G. Munhoz¹²¹,
 K. Mürning⁴⁵, R.H. Munzer⁷⁰, H. Murakami¹²⁹, S. Murray⁷⁶,
 L. Musa³⁵, J. Musinsky⁶⁵, C.J. Myers¹²⁴, J.W. Myrcha¹³⁸, D. Nag⁴,
 B. Naik⁴⁸, R. Nair⁸⁶, B.K. Nandi⁴⁸, R. Nania^{12,53}, E. Nappi⁵²,
 A. Narayan⁴⁸, M.U. Naru¹⁵, H. Natal da Luz¹²¹, C. Nattrass¹²⁷,
 S.R. Navarro², K. Nayak⁸⁸, R. Nayak⁴⁸, T.K. Nayak¹³⁷, S. Nazarenko¹⁰⁸,
 R.A. Negrao De Oliveira^{70,35}, L. Nellen⁷², S.V. Nesbo³⁷, F. Ng¹²⁴,
 M. Nicassio¹⁰⁶, M. Niculescu⁶⁸, J. Niedziela^{35,138}, B.S. Nielsen⁹¹,
 S. Nikolaev⁹⁰, S. Nikulin⁹⁰, V. Nikulin⁹⁶, F. Noferini^{12,53},
 P. Nomokonov⁷⁷, G. Nooren⁶³, J.C.C. Noris², J. Norman¹²⁶,
 A. Nyanin⁹⁰, J. Nystrand²², H. Oeschler^{19,104,i}, H. Oh¹⁴², A. Ohlson¹⁰⁴,
 T. Okubo⁴⁷, L. Olah¹⁴⁰, J. Oleniacz¹³⁸, A.C. Oliveira Da Silva¹²¹,
 M.H. Oliver¹⁴¹, J. Onderwaater¹⁰⁶, C. Oppedisano⁵⁸, R. Orava⁴⁶,
 M. Oravec¹¹⁶, A. Ortiz Velasquez⁷², A. Oskarsson³⁴, J. Otwinowski¹¹⁸,
 K. Oyama⁸⁴, Y. Pachmayer¹⁰⁴, V. Pacik⁹¹, D. Pagano¹³⁵, G. Paic⁷²,
 P. Palni⁷, J. Pan¹³⁹, A.K. Pandey⁴⁸, S. Panebianco⁷⁵, V. Papikyan¹,
 P. Pareek⁴⁹, J. Park⁶⁰, S. Parmar⁹⁹, A. Passfeld⁷¹, S.P. Pathak¹²⁴,
 R.N. Patra¹³⁷, B. Paul⁵⁸, H. Pei⁷, T. Peitzmann⁶³, X. Peng⁷,
 L.G. Pereira⁷³, H. Pereira Da Costa⁷⁵, D. Peresunko^{83,90},
 E. Perez Lezama⁷⁰, V. Peskov⁷⁰, Y. Pestov⁵, V. Petráček³⁹, V. Petrov¹¹²,
 M. Petrovici⁸⁷, C. Petta²⁸, R.P. Pezzi⁷³, S. Piano⁵⁹, M. Pikna³⁸,
 P. Pillot¹¹⁴, L.O.D.L. Pimentel⁹¹, O. Pinazza^{53,35}, L. Pinsky¹²⁴,
 D.B. Piyarathna¹²⁴, M. Płoskoń⁸², M. Planinic⁹⁸, F. Pliquett⁷⁰,
 J. Pluta¹³⁸, S. Pochybova¹⁴⁰, P.L.M. Podesta-Lerma¹²⁰,
 M.G. Poghosyan⁹⁵, B. Polichtchouk¹¹², N. Poljak⁹⁸, W. Poonsawat¹¹⁵,
 A. Pop⁸⁷, H. Poppenborg⁷¹, S. Porteboeuf-Houssais¹³¹, V. Pozdniakov⁷⁷,
 S.K. Prasad⁴, R. Preghenella⁵³, F. Prino⁵⁸, C.A. Pruneau¹³⁹,
 I. Pshenichnov⁶², M. Puccio²⁶, V. Punin¹⁰⁸, J. Putschke¹³⁹, S. Raha⁴,
 S. Rajput¹⁰¹, J. Rak¹²⁵, A. Rakotozafindrabe⁷⁵, L. Ramello³², F. Rami¹³³,
 D.B. Rana¹²⁴, R. Raniwala¹⁰², S. Raniwala¹⁰², S.S. Räsänen⁴⁶,
 B.T. Rascanu⁷⁰, D. Rathee⁹⁹, V. Ratza⁴⁵, I. Ravasenga³¹, K.F. Read^{127,95},
 K. Redlich^{86,v}, A. Rehman²², P. Reichelt⁷⁰, F. Reidt³⁵, X. Ren⁷,
 R. Renfordt⁷⁰, A. Reshetin⁶², K. Reygers¹⁰⁴, V. Riabov⁹⁶, T. Richert^{34,63},
 M. Richter²¹, P. Riedler³⁵, W. Riegler³⁵, F. Riggi²⁸, C. Ristea⁶⁸,
 M. Rodríguez Cahuantzi², K. Røed²¹, E. Rogochaya⁷⁷, D. Rohr^{35,42},
 D. Röhrich²², P.S. Rokita¹³⁸, F. Ronchetti⁵¹, E.D. Rosas⁷², P. Rosnet¹³¹,
 A. Rossi^{29,56}, A. Rotondi¹³⁴, F. Roukoutakis⁸⁵, C. Roy¹³³, P. Roy¹⁰⁹,

A.J. Rubio Montero¹⁰, O.V. Rueda⁷², R. Rui²⁵, B. Rumyantsev⁷⁷,
 A. Rustamov⁸⁹, E. Ryabinkin⁹⁰, Y. Ryabov⁹⁶, A. Rybicki¹¹⁸,
 S. Saarinen⁴⁶, S. Sadhu¹³⁷, S. Sadovsky¹¹², K. Šafařík³⁵, S.K. Saha¹³⁷,
 B. Sahlmuller⁷⁰, B. Sahoo⁴⁸, P. Sahoo⁴⁹, R. Sahoo⁴⁹, S. Sahoo⁶⁷,
 P.K. Sahu⁶⁷, J. Saini¹³⁷, S. Sakai¹³⁰, M.A. Saleh¹³⁹, J. Salzwedel¹⁸,
 S. Sambyal¹⁰¹, V. Samsonov^{96,83}, A. Sandoval⁷⁴, A. Sarkar⁷⁶,
 D. Sarkar¹³⁷, N. Sarkar¹³⁷, P. Sarma⁴⁴, M.H.P. Sas⁶³, E. Scapparone⁵³,
 F. Scarlassara²⁹, B. Schaefer⁹⁵, H.S. Scheid⁷⁰, C. Schiaua⁸⁷,
 R. Schicker¹⁰⁴, C. Schmidt¹⁰⁶, H.R. Schmidt¹⁰³, M.O. Schmidt¹⁰⁴,
 M. Schmidt¹⁰³, N.V. Schmidt^{95,70}, J. Schukraft³⁵, Y. Schutz^{35,133},
 K. Schwarz¹⁰⁶, K. Schweda¹⁰⁶, G. Scioli²⁷, E. Scomparin⁵⁸, M. Šefčík⁴⁰,
 J.E. Seger⁹⁷, Y. Sekiguchi¹²⁹, D. Sekihata⁴⁷, I. Selyuzhenkov^{106,83},
 K. Senosi⁷⁶, S. Senyukov¹³³, E. Serradilla^{74,10}, P. Sett⁴⁸, A. Sevcenco⁶⁸,
 A. Shabanov⁶², A. Shabetai¹¹⁴, R. Shahoyan³⁵, W. Shaikh¹⁰⁹,
 A. Shangaraev¹¹², A. Sharma⁹⁹, A. Sharma¹⁰¹, M. Sharma¹⁰¹,
 M. Sharma¹⁰¹, N. Sharma⁹⁹, A.I. Sheikh¹³⁷, K. Shigaki⁴⁷, S. Shirinkin⁶⁴,
 Q. Shou⁷, K. Shtejer^{9,26}, Y. Sibiriyak⁹⁰, S. Siddhanta⁵⁴, K.M. Sielewicz³⁵,
 T. Siemiarczuk⁸⁶, S. Silaeva⁹⁰, D. Silvermyr³⁴, G. Simatovic⁹²,
 G. Simonetti³⁵, R. Singaraju¹³⁷, R. Singh⁸⁸, V. Singhal¹³⁷, T. Sinha¹⁰⁹,
 B. Sitar³⁸, M. Sitta³², T.B. Skaali²¹, M. Slupecki¹²⁵, N. Smirnov¹⁴¹,
 R.J.M. Snellings⁶³, T.W. Snellman¹²⁵, J. Song¹⁹, M. Song¹⁴²,
 F. Soramel²⁹, S. Sorensen¹²⁷, F. Sozzi¹⁰⁶, I. Sputowska¹¹⁸, J. Stachel¹⁰⁴,
 I. Stan⁶⁸, P. Stankus⁹⁵, E. Stenlund³⁴, D. Stocco¹¹⁴, M.M. Storetvedt³⁷,
 P. Strmen³⁸, A.A.P. Suaide¹²¹, T. Sugitate⁴⁷, C. Suire⁶¹,
 M. Suleymanov¹⁵, M. Suljic²⁵, R. Sultanov⁶⁴, M. Šumbera⁹⁴,
 S. Sumowidagdo⁵⁰, K. Suzuki¹¹³, S. Swain⁶⁷, A. Szabo³⁸, I. Szarka³⁸,
 U. Tabassam¹⁵, J. Takahashi¹²², G.J. Tambave²², N. Tanaka¹³⁰,
 M. Tarhini⁶¹, M. Tariq¹⁷, M.G. Tarzila⁸⁷, A. Tauro³⁵, G. Tejada Muñoz²,
 A. Telesca³⁵, K. Terasaki¹²⁹, C. Terrevoli²⁹, B. Teyssier¹³², D. Thakur⁴⁹,
 S. Thakur¹³⁷, D. Thomas¹¹⁹, F. Thoresen⁹¹, R. Tieulent¹³²,
 A. Tikhonov⁶², A.R. Timmins¹²⁴, A. Toia⁷⁰, M. Toppi⁵¹, S.R. Torres¹²⁰,
 S. Tripathy⁴⁹, S. Trogolo²⁶, G. Trombetta³³, L. Tropp⁴⁰, V. Trubnikov³,
 W.H. Trzaska¹²⁵, B.A. Trzeciak⁶³, T. Tsuji¹²⁹, A. Tumkin¹⁰⁸,
 R. Turrisi⁵⁶, T.S. Tveter²¹, K. Ullaland²², E.N. Umaka¹²⁴, A. Uras¹³²,
 G.L. Usai²⁴, A. Utrobicic⁹⁸, M. Vala^{116,65}, J. Van Der Maarel⁶³,
 J.W. Van Hoorne³⁵, M. van Leeuwen⁶³, T. Vanat⁹⁴, P. Vande Vyvre³⁵,
 D. Varga¹⁴⁰, A. Vargas², M. Vargyas¹²⁵, R. Varma⁴⁸, M. Vasileiou⁸⁵,

A. Vasiliev⁹⁰, A. Vauthier⁸¹, O. Vázquez Doce^{105,36}, V. Vechernin¹³⁶,
 A.M. Veen⁶³, A. Velure²², E. Vercellin²⁶, S. Vergara Limón², R. Vernet⁸,
 R. Vértesi¹⁴⁰, L. Vickovic¹¹⁷, S. Vigolo⁶³, J. Viinikainen¹²⁵,
 Z. Vilakazi¹²⁸, O. Villalobos Baillie¹¹⁰, A. Villatoro Tello²,
 A. Vinogradov⁹⁰, L. Vinogradov¹³⁶, T. Virgili³⁰, V. Vislavicius³⁴,
 A. Vodopyanov⁷⁷, M.A. Völkl¹⁰³, K. Voloshin⁶⁴, S.A. Voloshin¹³⁹,
 G. Volpe³³, B. von Haller³⁵, I. Vorobyev^{105,36}, D. Voscek¹¹⁶,
 D. Vranic^{35,106}, J. Vrláková⁴⁰, B. Wagner²², H. Wang⁶³, M. Wang⁷,
 D. Watanabe¹³⁰, Y. Watanabe^{129,130}, M. Weber¹¹³, S.G. Weber¹⁰⁶,
 D.F. Weiser¹⁰⁴, S.C. Wenzel³⁵, J.P. Wessels⁷¹, U. Westerhoff⁷¹,
 A.M. Whitehead¹⁰⁰, J. Wiechula⁷⁰, J. Wikne²¹, G. Wilk⁸⁶,
 J. Wilkinson^{104,53}, G.A. Willems^{35,71}, M.C.S. Williams⁵³, E. Willsher¹¹⁰,
 B. Windelband¹⁰⁴, W.E. Witt¹²⁷, R. Xu⁷, S. Yalcin⁸⁰, K. Yamakawa⁴⁷,
 P. Yang⁷, S. Yano⁴⁷, Z. Yin⁷, H. Yokoyama^{130,81}, I.-K. Yoo¹⁹,
 J.H. Yoon⁶⁰, E. Yun¹⁹, V. Yurchenko³, V. Zaccolo⁵⁸, A. Zaman¹⁵,
 C. Zampolli³⁵, H.J.C. Zanolini¹²¹, N. Zardoshti¹¹⁰, A. Zarochentsev¹³⁶,
 P. Závada⁶⁶, N. Zaviyalov¹⁰⁸, H. Zbroszczyk¹³⁸, M. Zhalov⁹⁶,
 H. Zhang^{22,7}, X. Zhang⁷, Y. Zhang⁷, C. Zhang⁶³, Z. Zhang^{7,131},
 C. Zhao²¹, N. Zhigareva⁶⁴, D. Zhou⁷, Y. Zhou⁹¹, Z. Zhou²², H. Zhu²²,
 J. Zhu⁷, Y. Zhu⁷, A. Zichichi^{12,27}, M.B. Zimmermann³⁵, G. Zinovjev³,
 J. Zmeskal¹¹³, S. Zou⁷

¹ A.I. Alikhanyan National Science Laboratory (Yerevan Physics Institute) Foundation, Yerevan, Armenia

² Benemérita Universidad Autónoma de Puebla, Puebla, Mexico

³ Bogolyubov Institute for Theoretical Physics, Kiev, Ukraine

⁴ Bose Institute, Department of Physics and Centre for Astroparticle Physics and Space Science (CAPSS), Kolkata, India

⁵ Budker Institute for Nuclear Physics, Novosibirsk, Russia

⁶ California Polytechnic State University, San Luis Obispo, CA, United States

⁷ Central China Normal University, Wuhan, China

⁸ Centre de Calcul de l'IN2P3, Villeurbanne, Lyon, France

⁹ Centro de Aplicaciones Tecnológicas y Desarrollo Nuclear (CEADEN), Havana, Cuba

¹⁰ Centro de Investigaciones Energéticas Medioambientales y Tecnológicas (CIEMAT), Madrid, Spain

¹¹ Centro de Investigación y de Estudios Avanzados (CINVESTAV), Mexico City and Mérida, Mexico

¹² Centro Fermi – Museo Storico della Fisica e Centro Studi e Ricerche ‘Enrico Fermi’, Rome, Italy

¹³ Chicago State University, Chicago, IL, United States

¹⁴ China Institute of Atomic Energy, Beijing, China

¹⁵ COMSATS Institute of Information Technology (CIIT), Islamabad, Pakistan

¹⁶ Departamento de Física de Partículas and IGFAE, Universidad de Santiago de Compostela, Santiago de Compostela, Spain

¹⁷ Department of Physics, Aligarh Muslim University, Aligarh, India

¹⁸ Department of Physics, Ohio State University, Columbus, OH, United States

¹⁹ Department of Physics, Pusan National University, Pusan, Republic of Korea

²⁰ Department of Physics, Sejong University, Seoul, Republic of Korea

²¹ Department of Physics, University of Oslo, Oslo, Norway

²² Department of Physics and Technology, University of Bergen, Bergen, Norway

- 23 Dipartimento di Fisica dell'Università 'La Sapienza' and Sezione INFN, Rome, Italy
- 24 Dipartimento di Fisica dell'Università and Sezione INFN, Cagliari, Italy
- 25 Dipartimento di Fisica dell'Università and Sezione INFN, Trieste, Italy
- 26 Dipartimento di Fisica dell'Università and Sezione INFN, Turin, Italy
- 27 Dipartimento di Fisica e Astronomia dell'Università and Sezione INFN, Bologna, Italy
- 28 Dipartimento di Fisica e Astronomia dell'Università and Sezione INFN, Catania, Italy
- 29 Dipartimento di Fisica e Astronomia dell'Università and Sezione INFN, Padova, Italy
- 30 Dipartimento di Fisica 'E.R. Caianiello' dell'Università and Gruppo Collegato INFN, Salerno, Italy
- 31 Dipartimento DISAT del Politecnico and Sezione INFN, Turin, Italy
- 32 Dipartimento di Scienze e Innovazione Tecnologica dell'Università del Piemonte Orientale and INFN Sezione di Torino, Alessandria, Italy
- 33 Dipartimento Interateneo di Fisica 'M. Merlin' and Sezione INFN, Bari, Italy
- 34 Division of Experimental High Energy Physics, University of Lund, Lund, Sweden
- 35 European Organization for Nuclear Research (CERN), Geneva, Switzerland
- 36 Excellence Cluster Universe, Technische Universität München, Munich, Germany
- 37 Faculty of Engineering, Bergen University College, Bergen, Norway
- 38 Faculty of Mathematics, Physics and Informatics, Comenius University, Bratislava, Slovakia
- 39 Faculty of Nuclear Sciences and Physical Engineering, Czech Technical University in Prague, Prague, Czech Republic
- 40 Faculty of Science, P.J. Šafárik University, Košice, Slovakia
- 41 Faculty of Technology, Buskerud and Vestfold University College, Tonsberg, Norway
- 42 Frankfurt Institute for Advanced Studies, Johann Wolfgang Goethe-Universität Frankfurt, Frankfurt, Germany
- 43 Gangneung-Wonju National University, Gangneung, Republic of Korea
- 44 Gauhati University, Department of Physics, Guwahati, India
- 45 Helmholtz-Institut für Strahlen- und Kernphysik, Rheinische Friedrich-Wilhelms-Universität Bonn, Bonn, Germany
- 46 Helsinki Institute of Physics (HIP), Helsinki, Finland
- 47 Hiroshima University, Hiroshima, Japan
- 48 Indian Institute of Technology Bombay (IIT), Mumbai, India
- 49 Indian Institute of Technology Indore, Indore, India
- 50 Indonesian Institute of Sciences, Jakarta, Indonesia
- 51 INFN, Laboratori Nazionali di Frascati, Frascati, Italy
- 52 INFN, Sezione di Bari, Bari, Italy
- 53 INFN, Sezione di Bologna, Bologna, Italy
- 54 INFN, Sezione di Cagliari, Cagliari, Italy
- 55 INFN, Sezione di Catania, Catania, Italy
- 56 INFN, Sezione di Padova, Padova, Italy
- 57 INFN, Sezione di Roma, Rome, Italy
- 58 INFN, Sezione di Torino, Turin, Italy
- 59 INFN, Sezione di Trieste, Trieste, Italy
- 60 Inha University, Incheon, Republic of Korea
- 61 Institut de Physique Nucléaire d'Orsay (IPNO), Université Paris-Sud, CNRS-IN2P3, Orsay, France
- 62 Institute for Nuclear Research, Academy of Sciences, Moscow, Russia
- 63 Institute for Subatomic Physics of Utrecht University, Utrecht, Netherlands
- 64 Institute for Theoretical and Experimental Physics, Moscow, Russia
- 65 Institute of Experimental Physics, Slovak Academy of Sciences, Košice, Slovakia
- 66 Institute of Physics, Academy of Sciences of the Czech Republic, Prague, Czech Republic
- 67 Institute of Physics, Bhubaneswar, India
- 68 Institute of Space Science (ISS), Bucharest, Romania
- 69 Institut für Informatik, Johann Wolfgang Goethe-Universität Frankfurt, Frankfurt, Germany
- 70 Institut für Kernphysik, Johann Wolfgang Goethe-Universität Frankfurt, Frankfurt, Germany
- 71 Institut für Kernphysik, Westfälische Wilhelms-Universität Münster, Münster, Germany
- 72 Instituto de Ciencias Nucleares, Universidad Nacional Autónoma de México, Mexico City, Mexico
- 73 Instituto de Física, Universidade Federal do Rio Grande do Sul (UFRGS), Porto Alegre, Brazil
- 74 Instituto de Física, Universidad Nacional Autónoma de México, Mexico City, Mexico
- 75 IRFU, CEA, Université Paris-Saclay, Saclay, France
- 76 iThemba LABS, National Research Foundation, Somerset West, South Africa

- 77 *Joint Institute for Nuclear Research (JINR), Dubna, Russia*
- 78 *Konkuk University, Seoul, Republic of Korea*
- 79 *Korea Institute of Science and Technology Information, Daejeon, Republic of Korea*
- 80 *KTO Karatay University, Konya, Turkey*
- 81 *Laboratoire de Physique Subatomique et de Cosmologie, Université Grenoble-Alpes, CNRS-IN2P3, Grenoble, France*
- 82 *Lawrence Berkeley National Laboratory, Berkeley, CA, United States*
- 83 *Moscow Engineering Physics Institute, Moscow, Russia*
- 84 *Nagasaki Institute of Applied Science, Nagasaki, Japan*
- 85 *National and Kapodistrian University of Athens, Physics Department, Athens, Greece*
- 86 *National Centre for Nuclear Studies, Warsaw, Poland*
- 87 *National Institute for Physics and Nuclear Engineering, Bucharest, Romania*
- 88 *National Institute of Science Education and Research, HBNI, Jatni, India*
- 89 *National Nuclear Research Center, Baku, Azerbaijan*
- 90 *National Research Centre Kurchatov Institute, Moscow, Russia*
- 91 *Niels Bohr Institute, University of Copenhagen, Copenhagen, Denmark*
- 92 *Nikhef, Nationaal instituut voor subatomaire fysica, Amsterdam, Netherlands*
- 93 *Nuclear Physics Group, STFC Daresbury Laboratory, Daresbury, United Kingdom*
- 94 *Nuclear Physics Institute, Academy of Sciences of the Czech Republic, Řež u Prahy, Czech Republic*
- 95 *Oak Ridge National Laboratory, Oak Ridge, TN, United States*
- 96 *Petersburg Nuclear Physics Institute, Gatchina, Russia*
- 97 *Physics Department, Creighton University, Omaha, NE, United States*
- 98 *Physics Department, Faculty of Science, University of Zagreb, Zagreb, Croatia*
- 99 *Physics Department, Panjab University, Chandigarh, India*
- 100 *Physics Department, University of Cape Town, Cape Town, South Africa*
- 101 *Physics Department, University of Jammu, Jammu, India*
- 102 *Physics Department, University of Rajasthan, Jaipur, India*
- 103 *Physikalisches Institut, Eberhard Karls Universität Tübingen, Tübingen, Germany*
- 104 *Physikalisches Institut, Ruprecht-Karls-Universität Heidelberg, Heidelberg, Germany*
- 105 *Physik Department, Technische Universität München, Munich, Germany*
- 106 *Research Division and ExtreMe Matter Institute EMMI, GSI Helmholtzzentrum für Schwerionenforschung GmbH, Darmstadt, Germany*
- 107 *Rudjer Bošković Institute, Zagreb, Croatia*
- 108 *Russian Federal Nuclear Center (VNIIEF), Sarov, Russia*
- 109 *Saha Institute of Nuclear Physics, Kolkata, India*
- 110 *School of Physics and Astronomy, University of Birmingham, Birmingham, United Kingdom*
- 111 *Sección Física, Departamento de Ciencias, Pontificia Universidad Católica del Perú, Lima, Peru*
- 112 *SSC IHEP of NRC Kurchatov institute, Protvino, Russia*
- 113 *Stefan Meyer Institut für Subatomare Physik (SMI), Vienna, Austria*
- 114 *SUBATECH, IMT Atlantique, Université de Nantes, CNRS-IN2P3, Nantes, France*
- 115 *Suranaree University of Technology, Nakhon Ratchasima, Thailand*
- 116 *Technical University of Košice, Košice, Slovakia*
- 117 *Technical University of Split FESB, Split, Croatia*
- 118 *The Henryk Niewodniczanski Institute of Nuclear Physics, Polish Academy of Sciences, Cracow, Poland*
- 119 *The University of Texas at Austin, Physics Department, Austin, TX, United States*
- 120 *Universidad Autónoma de Sinaloa, Culiacán, Mexico*
- 121 *Universidade de São Paulo (USP), São Paulo, Brazil*
- 122 *Universidade Estadual de Campinas (UNICAMP), Campinas, Brazil*
- 123 *Universidade Federal do ABC, Santo Andre, Brazil*
- 124 *University of Houston, Houston, TX, United States*
- 125 *University of Jyväskylä, Jyväskylä, Finland*
- 126 *University of Liverpool, Liverpool, United Kingdom*
- 127 *University of Tennessee, Knoxville, TN, United States*
- 128 *University of the Witwatersrand, Johannesburg, South Africa*
- 129 *University of Tokyo, Tokyo, Japan*
- 130 *University of Tsukuba, Tsukuba, Japan*

- ¹³¹ *Université Clermont Auvergne, CNRS/IN2P3, LPC, Clermont-Ferrand, France*
¹³² *Université de Lyon, Université Lyon 1, CNRS/IN2P3, IPN-Lyon, Villeurbanne, Lyon, France*
¹³³ *Université de Strasbourg, CNRS, IPHC UMR 7178, F-67000 Strasbourg, France*
¹³⁴ *Università degli Studi di Pavia, Pavia, Italy*
¹³⁵ *Università di Brescia, Brescia, Italy*
¹³⁶ *V. Fock Institute for Physics, St. Petersburg State University, St. Petersburg, Russia*
¹³⁷ *Variable Energy Cyclotron Centre, Kolkata, India*
¹³⁸ *Warsaw University of Technology, Warsaw, Poland*
¹³⁹ *Wayne State University, Detroit, MI, United States*
¹⁴⁰ *Wigner Research Centre for Physics, Hungarian Academy of Sciences, Budapest, Hungary*
¹⁴¹ *Yale University, New Haven, CT, United States*
¹⁴² *Yonsei University, Seoul, Republic of Korea*
¹⁴³ *Zentrum für Technologietransfer und Telekommunikation (ZTT), Fachhochschule Worms, Worms, Germany*

- ⁱ Deceased.
ⁱⁱ Dipartimento DET del Politecnico di Torino, Turin, Italy.
ⁱⁱⁱ M.V. Lomonosov Moscow State University, D.V. Skobeltsyn Institute of Nuclear Physics, Moscow, Russia.
^{iv} Department of Applied Physics, Aligarh Muslim University, Aligarh, India.
^v Institute of Theoretical Physics, University of Wrocław, Poland.